Chalcogenide Letters Vol. 11, No. 3, March 2014, p. 121 - 128

STRUCTURAL, ELASTIC AND THERMODYNAMIC PROPERTIES OF ROCK-SALT STRUCTURE CdSe AT HIGH TEMPERATURE AND HIGH PRESSURE

H.J. HOU[a,*], J.W. YANG[b], F. HU[c], S.R. ZHANG[d], S.X. YANG[a]
[a]*School of Materials Engineering, Yancheng Institute of Technology, Yancheng 224051, China*
[b]*Department of Physics, Taiyuan Normal University, Taiyuan 030031, People's Republic of China*
[c]*School of Mathematic and Physical Science, Xuzhou Institute of Technology, Xuzh ou 221000, China*
[d]*Department of Physics and Information Engineering, Huaihua University, Huaihua 418008, China*

A theoretical study of the structural, elastic and thermodynamic properties of the rock-salt (RS) structure CdSe are presented in this paper by performing first principles calculations within local density approximation (LDA) based on Density Functional Theory (DFT). The values of lattice constant, bulk modulus and its pressure derivatives and elastic constants are in agreement with the available theoretical results. It is also found that the RS structure CdSe should be unstable above about 28 GPa. The pressure and temperature dependencies of the Heat capacity, Internal energy, Entropy, Helmholtz free energy, Grüneisen parameter, Thermal expansion coefficient and Debye temperature are obtained by the quasi-harmonic Debye model in the ranges of 0 - 1000 K and 0 - 28 GPa.

(Received January 12, 2014; Accepted March 3, 2014)

Keywords CdSe, Structural, Elastic constant, Thermodynamic properties

1. Introduction

The II-VI semiconductors, owing to their direct and wide band gap, are technologically important materials. The recent successful fabrication of the blue-green laser and light-emitting diodes based on these materials has renewed interest in their physical properties. Among these materials, CdSe has been reported early by several authors. It has attracted special attention in recent years for their applications in γ-ray detectors, infrared windows, solar cells and other optoelectronic devices. At ambient temperature and pressure, CdSe is found to crystallize in the hexagonal wurtzite (WZ) structure. The cubic analog of this is the metastable zinc-blend (ZB) structure, which can be grown using molecular beam epitaxy [1]. Under high pressure both structure transform into a phase with NaCl-type structure [2-4]. The ab initio calculations, as well as others or experiment, have been extensively used to carry out the structural [3, 5-6], band structure [6-8], elastic [9-11], lattice dynamical [12] and phase transition [2-4, 13-14] properties for CdSe. From the above, it is clear that exists many structure and phase transition calculations from WZ structure to RS structure CdSe crystal, but there are very few reported detail studies on the elastic and thermodynamic properties of RS structure CdSe at different pressures and temperatures. Therefore, the aim of this work is to give a detailed description of the behavior of elastic and thermodynamic properties of RS structure CdSe crystal by using the plane wave method and quasi-harmonic Debye model.

* Corresponding author: wyezhhj@126.com

2. Computational methods

The exchange correlation effects were taken into account within the Perdew-Wang (PW92) scheme [15] in the LDA pseudo-potential. And the plane wave basis set to the density functional theory is employed by the ABINIT Package [16-17].The self consistent norm-conserving pseudo-potentials were generated by using FHI98PP code [18] with the Troullier-Martins scheme [19].

For the characterization of the different properties, several sets of convergence tests have been carried out in order to choose correctly the grid of special *k* points and the plane wave kinetic energy cut-off. The chosen plane wave kinetic energy cut-off is 30 Hartree for RS structure CdSe. For the RS structure CdSe ,we adopt 4 × 4 × 4 shifted Monkhorst-Pack *k*-point.

3. Results and discussions

3.1 Structure properties of CdSe

For the RS structure CdSe, We calculated the total energy as a function of the unit-cell volume around the equilibrium cell volume V_0, which is illustrated in Fig.1. The calculated total energies are fitted to Birch-Murnaghan equation of state (EOS) [20] and Vinet EOS [21] to obtain an analytical interpolation of our computed points from which to calculate derived structural properties. The obtained equilibrium lattice constant a, zero-pressure bulk modulus B_0 and its pressure derivation $B_0^{'}$ and $B_0^{''}$ from the Birch-Murnaghan EOS and Vinet EOS are listed in table 1, together with other theoretical results [3,6, 22-23, 25]. It can be seen from table1 that the lattice constant for RS structure CdSe is 5.6315 Å, the bulk modulus for the RS structure CdSe is B_0 = 74.44 GPa and its pressure derivative are $B_0^{'}$ = 4.9395 and $B_0^{''}$ = -0.0767 respectively. Obviously, the bulk modulus of 74.44 GPa is significantly smaller than the bulk modulus of 84.32 GPa, which was reported for the RS structure CdSe using the full-potential linear muffin-tin-orbital method (FP-LMTO) [3]. But the bulk modulus is close to the calculated value using the ab initio pseudopotential method with the LDA [6]. Moreover, comparing with other theoretical results, one can also see that the results from the Birch-Murnaghan EOS seem to be better than those from the Vinet EOS. So, the results from Birch-Murnaghan EOS are adopted in the following calculations.

Table 1. Lattice constant (Å), bulk modulus (GPa) and pressure derivative of bulk modulus of the RS structure CdSe

	This work		Other theoretical calculations					
RS								
a	5.6315 [a]	5.6316[b]	5.5762[c]	5.514[d]	5.586[d]	5.573[e]	5.717[e]	5.71[f]
5.72[h]								
B_0	74.44 [a]	73.98[b]	84.32[c]	74[d]	78[d]	74.1[e]	64.3 [e]	74±
2[g] 57.7[h]								
$B_0^{'}$	4.9395 [a]	5.0476[b]	4.8022[c]			10.7 [e]	5.1 [e]	
$B_0^{''}$	-0.0767 [a]	-0.1131[b]						

[a]Ref.[20]. [b]Ref. [21]. [c]Ref. [3]. [d]Ref. [6] . [e]Ref. [22]. [f]Ref. [23]. [g]Ref. [24]. [h]Ref. [25].

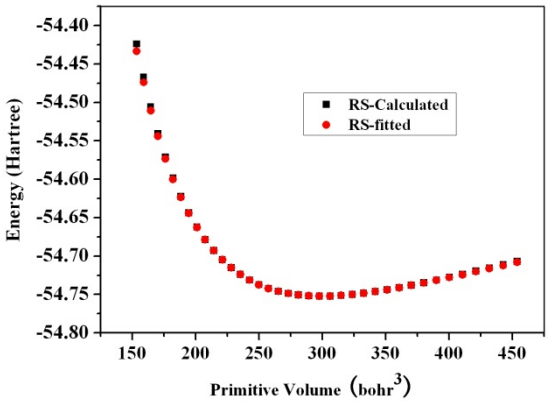

Fig. 1. Energy as a function of primitive cell volume for CdSe

3.2 The elastic properties

The elastic property plays an important part in providing valuable information about the mechanical and dynamical properties of solids, and give important information concerning the nature of the forces operating in solids. For instance, the inter-atomic potentials and EOS. The elastic property is also thermodynamically related to Debye temperature. The elastic constants can predict the structural stability of the materials. To gain a further insight into the mechanical stability of CdSe, we have calculated the elastic constants of RS structure by computing the change in energy of CdSe under small volume-conserving strains. The theoretical results are given in table 2. It is worth pointing out that the our theoretical calculations of the elastic constants for RS structure CdSe are in agreement with other theoretical reports [22, 25]. From table 2, we can also see that the calculated three independent elastic constants (C_{11}, C_{12}, C_{44}) of CdSe are found to be positive and satisfy the mechanical stability criteria [26]. Therefore, the RS structure CdSe is stable at zero temperature and below pressure 28 GPa .

$\tilde{C}_{44} \rangle 0 \qquad \tilde{C}_{11} \rangle |\tilde{C}_{12}| \qquad \tilde{C}_{11} + \tilde{C}_{12} \rangle 0$

Where $\tilde{C}_{\alpha\alpha} = C_{\alpha\alpha} - p \quad (\alpha = 1, 4) \qquad \tilde{C}_{12} = C_{\alpha\alpha} + p$

The condition $\tilde{C}_{44} \rangle 0$ is not satisfied when the pressure is above 28 GPa which means RS structure CdSe is mechanically unstable above 28 GPa. The pressure induced structural phase transformation from the RS structure to the Cmcm structure CdSe reported by N. Benkhettou et al. occurs at 20.1 GPa [3]. The experimental pressure of the NaCl to Cmcm structure transition is 27.0 GPa [27]. Our result is consistent with experimental data. Unfortunately, to our knowledge, no theoretical values and experimental data of elastic constants under high pressure are available for our comparison.

Table 2. Elastic constants C_{11}, C_{12} ,C_{44} (GPa) and elastic compliance coefficients S_{11}, S_{12}, S_{44} (10^{-2} GPa^{-1}) of RS structure CdSe at various pressures (GPa) at zero temperature (K)

Phase	Pressure(GPa)	C_{11}	C_{12}	C_{44}	S_{11}	S_{12}	S_{44}
RS							
0	133.0857	44.7621	28.9676	0.9045	-0.2277	3.4521	
	79.7[a]	46.7[a]	46.5[a]				
137.2[b]	49.4[b]	26.2[b]					
	94.3 [b]	40.6 [b]	25.7 [b]				
5	175.1967	51.8977	29.6936	0.6584	-0.1493	3.3677	
10	214.0065	56.7715	29.3554	0.5258	-0.1102	3.4065	
15	253.9813	62.5284	29.5377	0.4361	-0.0862	3.3855	
20	290.3923	67.6126	29.1436	0.3776	-0.0713	3.4313	
25	324.6417	71.5165	27.6145	0.3346	-0.0604	3.6213	
28	346.4154	74.8932	27.7341	0.3127	-0.0556	3.6057	

[a] Ref.[25]. [b] Ref.[22].

Finally, we have also calculated the elastic compliance coefficients S_{11}, S_{12} and S_{44} and the propagation velocity of longitudinal and transverse waves for CdSe crystal. S_{11}, S_{12} and S_{44} are obtained by the relatio ships $C_{44} = 1/S_{44}$, $C_{11} - C_{12} = (S_{11} - S_{12})^{-1}$, $C_{11} + 2C_{12} = (S_{11} - 2S_{12})^{-1}$ in the cubic system. In the cubic system the propagation velocity of longitudinal waves in [100], [110] and [111] directions are given as [28-29], ρ is the density of material.

$$V_L([100]) = \sqrt{C_{11}/\rho}$$

$$V_L([110]) = \sqrt{\frac{1}{2}(C_{11} + C_{12} + 2C_{44})/\rho}$$

$$V_L([111]) = \sqrt{\frac{1}{3}(C_{11} + 2C_{12} + 4C_{44})/\rho}$$

The propagation velocity in the transverse mode is expressed by

$$V_{T1}([100]) = V_{T2}([100]) = \sqrt{C_{44}/\rho}$$

$$V_{T1}([110]) = \sqrt{\frac{1}{2}(C_{11} - C_{12})/\rho}$$

$$V_{T2}([110]) = \sqrt{C_{44}/\rho}$$

$$V_{T1}([111]) = V_{T2}([111]) = \sqrt{\frac{1}{3}(C_{11} - C_{12} + C_{44})/\rho}$$

The theoretical results are listed in table 3. Unfortunately, as far as we know, there are no experimental and theoretical data available related to elastic compliance coefficients and propagation velocity of longitudinal and transverse waves of RS structure CdSe in the literature for our comparison.

Table3. The values of longitudinal (V_L) and two shear wave (V_{TI}, V_{T2}) velocities (km/s) in three directions at pressures ranging from 0 to 28 GPa and at zero temperature (K).

Pressure(GPa)		[100]			[110]			[111]	
	V_L	V_{T1}	V_{T2}	V_L	V_{T1}	V_{T2}	V_L	V_{T1}	V_{T2}
0	4.3242	2.0172	2.0172	4.0699	2.4910	2.0172	3.9815	1.3532	1.3532
5	4.8193	1.9840	1.9840	4.3576	2.8588	1.9840	4.1925	1.5012	1.5012
10	5.2053	1.9279	1.9279	4.5671	3.1550	1.9279	4.3335	1.6202	1.6202
15	5.5633	1.8972	1.8972	4.7838	3.4154	1.8972	4.4940	1.7298	1.7298
20	5.8514	1.8537	1.8537	4.9540	3.6240	1.8537	4.6162	1.8167	1.8167
25	6.0977	1.7784	1.7784	5.0842	3.8073	1.7784	4.6980	1.8901	1.8901
28	6.2488	1.7676	1.7676	5.1837	3.9119	1.7676	4.7762	1.9360	1.9360

3.3 Thermodynamic properties

The thermodynamic properties of solid material at high pressure and high temperature is an interesting topic in condensed matter physics [30-32]. In order to obtain the pressure and temperature influence on the thermodynamic properties, the quasi-harmonic Debye model [33] allowing for the phononic effects is applied.

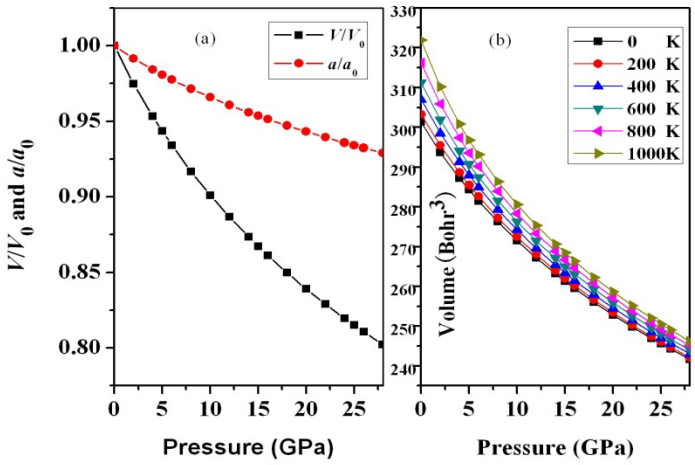

Fig. 2. Relative volume and Relative lattice constant versus pressure of the RS structure CdSe at 0 K (a) , volume versus pressure at different temperatures (b)

The pressure dependence of the a/a_0 (a is the lattice constant at pressure P and a_0 is the zero pressure lattice constant) and the relative volume V/V_0 (V is the volume of the unit cell at pressure P and V_0 is the zero pressure equilibrium volume) are illustrated in Fig. 2(a). The relative a/a_0 and volume V/V_0 decrease as the pressure enhances. The EOS of RS structure CdSe are ploted in Fig. 2(b), it can be found that the volume decreases with pressure at different temperatures.

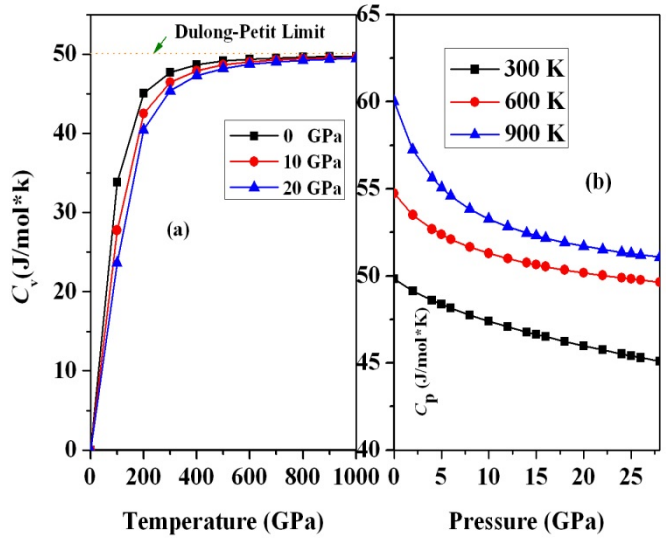

Fig. 3 The temperature dependence of heat capacity at constant volume and the pressure dependence of heat capacity at constant pressure.

Fig. 3(a) shows the calculated heat capacity at constant volume for different pressures as functions of the temperature. It can be seen from Fig.3(a) that the heat capacity C_V increases exponentially with the temperature at T < 500 K. But at high temperature, it follows the Debye model and approaches the Dulong-Petit limit indicating the thermal energy at high temperature excites all phonon modes. It is also clear that the increasing tendency of the heat capacity C_V as a function of temperature at 0, 10 and 20 GPa are, to some extent, very similar. Fig. 3(b) shows the heat capacity at different temperatures as a function of the pressure. Our calculation show that the temperature and pressure have opposite influences on the heat capacity C_P, the C_P increases with temperature and decreases with pressure, and the effect of temperature on the heat capacity C_P is more significant than that of pressure.

Table 4. The calculated Internal energy U (kJ/ mol), heat capacity of constant volume C_V (J /mol K), Heat capacity at constant pressure C_P (J /mol* K), Helmholtz free energy A (kJ/ mol), Entropy S (J /mol* K), Debye temperatureΘ (K), Grüneisen parameter γ and thermal expansion coefficient α (10^{-5}/K) for RS structure CdSe at 400 K under different pressures.*

P/GPa	*U*	C_V	*C*p	*A*	*S*	Θ	γ	α
0.00	20.44	48.70	51.77	-13.59	85.07	279.10	2.42	6.51
2.00	20.51	48.53	50.99	-12.23	81.84	298.31	2.31	5.52
4.00	20.57	48.37	50.43	-11.08	79.13	315.44	2.22	4.81
5.00	20.60	48.29	50.20	-10.57	77.92	323.42	2.19	4.52
6.00	20.63	48.21	49.99	-10.09	76.81	331.00	2.15	4.27
8.00	20.69	48.08	49.63	-9.21	74.76	345.38	2.10	3.86
10.00	20.75	47.94	49.32	-8.43	72.95	358.63	2.05	3.52
12.00	20.81	47.80	49.04	-7.71	71.29	371.32	2.00	3.24
14.00	20.86	47.67	48.80	-7.07	69.82	382.87	1.96	3.01
15.00	20.89	47.61	48.69	-6.76	69.12	388.57	1.95	2.91
16.00	20.91	47.55	48.57	-6.46	68.43	394.27	1.93	2.81
18.00	20.96	47.43	48.38	-5.91	67.20	404.62	1.90	2.64
20.00	21.01	47.30	48.18	-5.39	66.01	414.92	1.87	2.48
22.00	21.06	47.19	48.01	-4.91	64.93	424.46	1.85	2.35
24.00	21.11	47.07	47.84	-4.45	63.90	433.82	1.82	2.23
25.00	21.14	47.01	47.76	-4.22	63.40	438.47	1.81	2.18
26.00	21.16	46.96	47.68	-4.02	62.95	442.75	1.80	2.13
28.00	21.21	46.85	47.53	-3.61	62.04	451.40	1.78	2.03

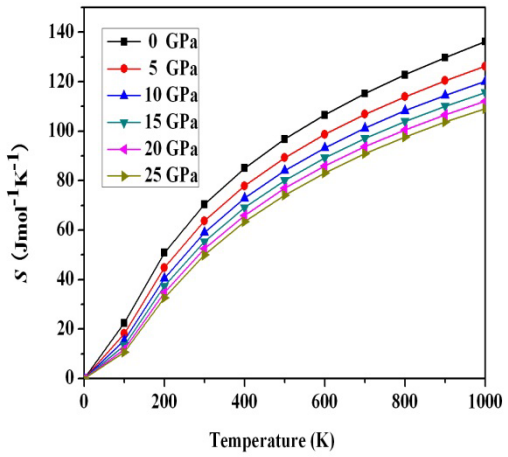

Fig. 4. Variation of entropy S with temperature T at P = 0, 5, 10, 15, 20 and 25 GPa, respectively

The entropy *S* dependence of temperature *T* at various pressures (0,5,10,15,20,25 GPa) are plotted in Fig.4. It is found that at fixed pressure *P*, the entropy *S* increases mostly exponentially with the temperature *T*. It can also be found that the effects of temperature on entropy *S* are more important at high temperature *T* than at low temperature *T*.

In addition, we have also calculated the internal energy *U*, entropy *S*, Helmholtz free energy *A* , Debye temperature Θ and Grüneisen parameter γ of CdSe at high temperature and high pressure. The calculated results are presented in table 4. We have not found any measurement about thermodynamic properties of RS structure CdSe at high temperature and high pressure for our comparison, therefore our calculations are useful for providing the thermodynamic properties of CdSe in RS structure.

4. Conclusion

In summary, the structural, elastic and thermodynamic properties of the RS structure CdSe at different pressures and temperatures are investigated by using ab initio plane wave pseudo-potential density functional theory within the LDA. The calculated results are in excellent agreement with the available theoretical results. It is found that the RS structure CdSe should be unstable above 28 GPa. The thermodynamic properties of RS structure CdSe are calculated by using the quasi-harmonic Debye model.The pressure and temperature dependencies of the Heat capacity, Internal energy, Entropy, Helmholtz free energy, Grüneisen parameter, Thermal expansion coefficient and Debye temperature are obtained systematically.

Acknowledgments

The project was supported by Open Project of Key Laboratory for Ecological-Environment Materials of Jiangsu Province (Grant no. EML2012011) and supported by research fund of Key Laboratory for Advanced Technology in Environmental Protection of Jiangsu Province (Grant no. AE201313)

References

[1] N. Samarth, H. Luo, J. K. Furdyna, S. B. Qadri, Y. R. Lee, A. K. Ramdas, N. Otsuka, Appl. Phys. Lett. **54**, 2680 (1989)
[2] Clive Bealing, Roman Martoňák,Carla Molteni , J. Chem. Phys. **130** ,124712 (2009)
[3] N. Benkhettou, D. Rached, B. Soudini, M. Driz ,phys. stat. sol. (b) **241**,101 (2004)
[4] Fuyuki Shimojo, Sanjay Kodiyalam,Ingvar Ebbsjö, Rajiv K. Kalia, Aiichiro Nakano, Priya Vashishta, Phys. Rev. B **70 ,**184111 (2004)
[5] S. Wei, S.B. Zhang, Phys. Rev. B **62**, 6944 (2000)
[6] Oleg Zakharov , Angel Rubio , Marvin L. Cohen, Phys. Rev. B **51**, 4926 (1995)
[7] Phillip Cervantes ,Quentin Williams, Michel Côté, Oleg Zakharov, Marvin L. Cohen, Phys. Rev. B **54**,17585 (1996)
[8] T.k.Bergstresser , Marvin L.Cohen ,Physics review **164**, 1069 (1967)
[9] Carl F. Cline, Harold L. Dunegan, Glenn W. Henderson , J. Appl. Phys. **38**, 1944 (1967)
[10] B. Bonello, B. Fernandez, J. Phys. Chem. Solids **54**, 209 (1993)
[11] D. Berlincourt, H Jaffe, LR Shiozawa , Physical Review **129**, 1009 (1963)
[12] F. Widulle, S. Kramp, N.M. Pyka, A. Göbel , T. Ruf , A. Debernardi , R. Lauck , M. Cardona Physica B**263** , 448 (1999)
[13] Heidrun Sowa ,Solid State Sci. **7**,1384 (2005)
[14] Dirk Zahn, Yuri Grin, Stefano Leoni , Phys. Rev. B, **72**, 064110 (2005)
[15] J. P. Perdew and Y. Wang, Phys. Rev. B, **45**, 13244 (1992)
[16] The ABINIT code is a common project of the Universite Catholique de Louvain, Corning Incorporated, and other contributors , <http://www.abinit.org>.
[17] X.Gonze, J.M.Beuken, R. Caracas, F. Detraux, M. Fuchs, G.M. Rignanese, L. Sindic, M.Verstraete, G.Zerah, F.Joller, M.Torrent, A.Roy, M.Mikami, P.h. Ghosez, J.Y. Raty, D.C.Allan, Comput. Mater. Sci. **25**, 478 (2002)
[18] M. Fuchs, M. Scheffler, Comput. Phys. Commun. **119**, 67 (1999)
[19] N. Troullier, J.L. Martins, Phys. Rev. B **43**,1993 (1991)
[20] J.P. Poirier, Introduction to the Physics of the Earth's Interior, Cambridge University Press, 1991.
[21] P. Vinet, J.H. Rose, J. Ferrante, J.R. Smith, J. Phys. Condens. Matter. **1**,1941 (1989)
[22] J.J. Tan, Y. Cheng , W.J. Zhu, Q.Q. Gou , Commun. Theor. Phys. **50**,220 (2008)
[23] J. N. Wickham, A. B. Herhold, A. P. Alivisatos, Phys. Rev. Lett. **84**, 923 (2000)
[24] S.H. Tolbert , A.P. Alivisatos, J. Chem. Phys. **102**, 4648 (1995)
[25] E. Rabani, J. Phys. Chem. **116**, 258 (2002)
[26] G.V. Sinko, N.A. Smirnow, J. Phys. Condens. Matter **14**, 6989 (2002)

[27] R. J. Nelmes, M. I. McMahon, in: High Pressure in Semiconductor Physics, edited by T. Suski and W. Paul (Academic Press, New York, 1998).
[28] www.ioffe.rssi.ru/SVA/NSM/Semicond/Si/mechanic.html
[29] D.H. Ren, X.L. Cheng, Chin. Phys. B , **21**, 127103 (2012)
[30] FJ. Kong, Y.F. Hu, Y.Z. Wang, B.L.Wang , L.J. Tang , Comp. Mater. Sci. **65**, 247 (2012)
[31] F.J. Kong, Y.H. Liu, B.L. Wang, Y.Z.Wang, Y.F. Hu, L.L.Wang, L.J. Tang , Physica B **407**, 2272 (2012)
[32] H.J. Hou , S.F. Zhu , B.J. Zhao , Y.Yu , S.R. Zhang , L.H.Xie, Physica B **407**, 408 (2012)
[33] M.A.Blanco, E.Francisco, V.Luana. Comput.Phys.Commun. **158** ,57 (2004)